CHAPTER 3: LITERATURE REVIEW – CONSTITUTIVE MODELLING OF SAND

3.1 INTRODUCTION

Constitutive models provide a simulation of material behaviour over the elastic and plastic states, when acted upon by sets of stresses. For soil, the behaviour of interest relates to volume changes in the material and the availability of strength of the soil matrix. This Chapter reviews constitutive models for sand, as a sand was used in the buried pipe trench installations, which form the basis of this thesis. An engineering description of the sand is provided in Chapter 4. Further description of the sand is given in Chapter 5, wherein the results of a range of engineering tests are presented, sufficient to form the basis for a constitutive model.

Constitutive models for clean sands differ from those for clay soils. This difference has been noted previously by researchers who found that the packing of a sand generally dictates its behaviour. A densely packed sand material acts differently from the same material when it is in a loose state. For all intents and purposes, loose sand may be treated as a different soil from dense sand, although the mineralogy and particle size distributions are the same for each soil. A constitutive model must be applicable for a sand material, regardless of its particle packing. Many researchers have therefore been searching for a suitable constitutive model for sand.

A special feature in the behaviour of a granular material such as sand is that shearing can produce dilation or increase in volume of the soil. Potential dilation generally affects shear capacity.

This chapter deals with the following subjects related to constitutive modelling of sand;

- Bulk and Shear Modulus
- Friction and Dilation
- Yield Surfaces
- Plastic Potentials and Flow Rules

- State Parameter
- Constitutive Models employing State Parameter.

3.2 BULK AND SHEAR MODULUS

It has been understood for some time now that the modulus of elasticity of a soil is not necessarily a constant, but varies with the stresses imposed on the soil. Holubec (1968) claimed that Boussinesq had understood this in 1876.

Janbu (1963) set out to explore the relationship between modulus of elasticity and stress for a wide range of different soils. Triaxial tests and one-dimensional oedometer tests were used to establish empirical relationships for each broad soil type. In the triaxial tests, the ratio of applied effective horizontal to effective vertical stress, K′, was kept constant throughout the test. In the oedometer test, the stress ratio is also constant, being equal to the 'at rest' earth pressure coefficient for the soil, K_o, since lateral strains are zero in the conventional oedometer.

Janbu based his empirical expression on a tangent modulus defined as:

$$M = \frac{d\sigma_1'}{d\varepsilon_1} = \frac{E}{1 - 2\nu\left(\frac{\sigma_1'}{\sigma_3'}\right)} \qquad 3\text{-}1$$

where E = Young's modulus of the soil

ν = Poisson's ratio of the soil

σ_1' = the major principal effective stress

σ_3' = the minor principal effective stress

and ε_1 = axial strain

The general empirical expression for all soils took the form:

$$M = mp_a \left[\frac{\sigma_1'}{p_a} \right]^{(1-a)} \qquad 3\text{-}2$$

where, p_a = atmospheric pressure

and m and a = soil dependent coefficients, which varied with soil porosity

Exponent 'a' can vary between unity and zero. Typical values of the coefficients for medium dense fine sand (40% porosity) are, a ≅ 0.5 and m ≅ 170. Normally consolidated clay was found to have a zero value for a.

Figure 3-1 from Janbu (1963) illustrates the dependence of the coefficients on soil porosity, n. K′ in the furthermost right diagram of the three original Janbu figures, which is entitled "B. FINE SAND", is the stress ratio, σ'_3/σ'_1. It is seen that Janbu's 'modulus number', m, decreased markedly with increase of porosity. An increase of soil porosity increases the at rest earth pressure coefficient, K_o, assuming Jaky's equation for normally consolidated sand (1944, as cited by Barnes 2000) applies. The dependence of the modulus number on porosity was however influenced by the chosen stress path. In the one dimensional oedometer test, K_o is constant for a particular porosity, but will change with change in the porosity. In the other tests, K′ was fixed and independent of porosity. The latter tests resulted in a higher rate of increase of m with porosity, n.

The usefulness of Janbu's power law formulation is somewhat limited owing to the dependence of the "constants" on the density of the soil. Pestana and Whittle (1995) demonstrated also that such models were only useful over one log cycle (base 10) of effective stress, as the mean stress exponent varied from a third to one, going from low to high stress levels.

In current constitutive models, such as those developed in the framework of Critical State Mechanics, a bulk modulus, K, and shear modulus, G, are the preferred volumetric parameters for soil. These moduli are defined over the elastic range of behaviour by Wood (1990) as:

$$K = \frac{dp}{d\varepsilon_p} = \frac{E}{3(1-2\nu)} \qquad 3\text{-}3$$

and

$$G = \frac{dq}{d\varepsilon_q} = \frac{E}{2(1+\nu)} \qquad 3\text{-}4$$

where p = mean stress = $\frac{\sigma_1' + 2\sigma_3'}{3}$, for triaxial shear conditions

ε_p = volumetric strain = $\varepsilon_1 + 2\varepsilon_3$ for triaxial shear conditions

q = deviatoric stress = $(\sigma_1' - \sigma_3')$, for triaxial shear conditions

ε_q = deviatoric strain = $\frac{2}{3}(\varepsilon_1 - \varepsilon_3)$, for triaxial shear conditions.

Janbu's tangent modulus can be seen to be directly proportional to either the bulk modulus or the shear modulus. Therefore, it may be expected that a similar form of empirical expression may be applied to either G or K, with a modified coefficient, m, which could be based on estimates of stress ratio and Poisson's ratio.

Janbu demonstrated in his experiments that modulus is stress dependent. As he kept constant the stress ratio, K′, the mean stress remained proportional to the major principal stress in each test. Hence it follows that modulus is dependent upon mean stress, p′. Janbu's empirical expression can be re-arranged to show this relationship, i.e.;

$$M = mp_a \left[\frac{p'}{p_a}\right]^{(1-a)} \left(\frac{3}{(1+2K')}\right)^{(1-a)} \qquad 3\text{-}5$$

or

$$M = mkp_a \left(\frac{p'}{p_a}\right)^{(1-a)} \qquad 3\text{-}6$$

where, k = a constant for constant stress ratio

and p_a = atmospheric pressure

Re-arranging the above expression for bulk modulus, K, the equation becomes:

$$K = \left[mp_a \left(\frac{p'}{p_a} \right)^{1-a} \right] \left[\frac{3}{(1+2K')} \right]^{1-a} \left[\frac{1-2\nu K'}{3(1-2\nu)} \right] \qquad 3\text{-}7$$

Kerisel (1963) reported the dependence of tangent Young's modulus, E, of Loire sand, both on mean stress, p′, and on the ratio of the current deviator stress to the deviator stress at failure, q/q_f. Figure 3-2 provides a family of curves for the sand tested at various mean stress levels and plotted as E against q/q_f. Modulus is seen to increase with mean stress, but decreased as q approaches q_f.

Holubec (1968) reported on the elastic and anisotropic behaviour of fully saturated, Ottawa sand. The sand was prepared at density indices of 40, 70 and 95%, approximately. Samples were tested in a triaxial cell in three different ways:

- constant cell pressure
- constant mean stress
- anisotropic consolidation ($K' \neq 1$).

For the axi-symmetrical conditions of the triaxial test, Holubec considered two values of Young's modulus and Poisson's ratio, E_1 and E_3, and ν_1 and ν_3, depending upon the direction considered. The two moduli were defined by the equations:

$$E_1 = \frac{d\sigma'_1 - 2\nu_3 d\sigma'_3}{d\varepsilon_1} \qquad 3\text{-}8$$

$$E_3 = \frac{d\sigma'_3 - \nu_3 d\sigma'_3 - \nu_1 d\sigma'_1}{d\varepsilon_3} \qquad 3\text{-}9$$

where E_1 = the axial elastic modulus in the direction of the major principal effective stress, σ'_1

E_3 = the axial elastic modulus in the direction of the minor principal effective stress, σ'_3

ν_1, ν_3 = Poisson's ratio in the direction of the major and minor principal directions, respectively

ε_1, ε_3 = strain in the direction of the major and minor principal directions, respectively

Young's modulus, E_1, was found to vary with the initial void ratio and the stresses, q and p′. A typical plot is given in Figure 3-3 of contours of E_1 in q-p′ space for Ottowa sand. The sand was prepared at a single value of initial density. Shearing was found to produce an anisotropic response in which E_1 became greater than E_3.

Lade and Nelson (1987) proposed a theoretical model for estimation of changes in Young's Modulus for a stressed sand mass. In this model, isotropic behaviour was assumed. Lade and Nelson's equation for modulus relied on the stress invariants, I_1 and J_2', where,

$$I_1 = 3p' \tag{3-10}$$

and

$$J_2' = 1/6\,[(\sigma_x - \sigma_y)^2 + (\sigma_y - \sigma_z)^2 + (\sigma_z - \sigma_x)^2] + \tau_{xy}^2 + \tau_{yz}^2 + \tau_{zx}^2 \tag{3-11}$$

Young's modulus could then be estimated by the equation,

$$E = M(p_a)\left[\left(\frac{I_1}{p_a}\right)^2 + R\left(\frac{J_2'}{p_a^2}\right)\right]^{\lambda} \tag{3-12}$$

where, p_a = atmospheric pressure

$$R = 6\frac{(1+\nu)}{1-2\nu}$$

M and λ are coefficients, which vary with soil density.

These researchers recommended performing drained, "conventional" triaxial tests with frequent unloading and loading to evaluate the coefficients, M and λ. Table 3-I provides typical values of these coefficients as well as Poisson's ratio, ν, for Santa Monica sand. In this same table, coefficients for Ottawa sand are given, which were taken from Dakoulas and Sun (1992).

Interest in the interpretation of the self-boring pressuremeter in sand has prompted a number of researchers to investigate a model for the small strain, shear modulus, G_o. Yu, Schnaid and Collins (1996) quoted Richart et al's (1970) general expression for G_o, as,

$$\frac{G_o}{p_a} = S\left(\frac{p'}{p_a}\right)^n \frac{(e_g - e)^2}{1+e} \qquad 3\text{-}13$$

where, e = the current void ratio

Both the material constants, S and e_g were found to be dependent on particle shape as is indicated in Table 3-II.

Fahey (1991) reported the parameters for the small strain shear modulus of Toyoura sand as being 900, 0.4 and 2.17 for S, n and e_c, respectively. Sasitharan, Robertson, Sego and Morgenstern (1994) described Toyoura sand as rounded to sub-rounded and containing feldspar to 25% by mass.

The formulation for the initial shear modulus is similar to that presented by Janbu (1963) for tangent modulus, M, but the effect of void ratio (or soil porosity) has been included in the equation.

Fahey and Carter (1993) adopted Yu and Richart's (1984) expression for G_o, which included an influence of shear stress on the modulus:

$$\frac{G_o}{p_a} = C\left(\frac{p'}{p_a}\right)^n \left(1 - \mu K_n^{\beta}\right) \qquad 3\text{-}14$$

where

$$K_n = \left(\frac{\sigma_1'/\sigma_3' - 1}{\left(\sigma_1'/\sigma_3'\right)_{max} - 1}\right) \qquad 3\text{-}15$$

and

$$C = S\left(\frac{(e_g - e)^2}{1+e}\right) \qquad 3\text{-}16$$

Values of the material constants, μ and β, of 0.3 and 1.5 were recommended by Yu and Richart (1984).

Fahey and Carter (1993) proposed that for plane strain conditions, the current secant shear modulus, G_s, may be described by the semi-empirical expression:

$$\frac{G_s}{G_o} = \frac{1}{\left(1+\frac{\gamma}{\gamma_r}\right)} = 1 - \frac{\tau}{\tau_{max}} \qquad 3\text{-}17$$

where γ = shear strain

γ_r = reference shear strain

$$= \frac{\tau_{max}}{G_o}$$

τ = shear stress

τ_{max} = maximum shear stress

The equation was further generalized to allow for fitting of experimental data through the constants, f and g:

$$\frac{G_s}{G_o} = 1 - f\left(\frac{\tau}{\tau_{max}}\right)^g \qquad 3\text{-}18$$

The tangent shear modulus may be found by differentiation of the above expression. The full formulation for the current shear modulus then takes into account the soil state or density, the mean stress level and principal stress ratios, and the proximity of the soil to failure. Therefore it satisfies the major variables influencing modulus that were identified by Holubec (1968).

The Fahey and Carter model was generalized for three-dimensional stress conditions by Lee and Salgado (2000), resulting in the following expression for the secant shear modulus:

$$\frac{G_s}{G_o} = \left[1 - f\left(\frac{\sqrt{J}_2 - \sqrt{J}_{2o}}{\sqrt{J}_{2max} - \sqrt{J}_{2o}}\right)^g\right]\left(\frac{I_1}{I_{1o}}\right)^{n_g} \qquad 3\text{-}19$$

where, the exponents, g and n_g, and the factor, f, are all material constants,

and $I_1 = 3p'$

$J_2 = 1/6\ [(\sigma'_1 - \sigma'_2)^2 + (\sigma'_2 - \sigma'_3)^2 + (\sigma'_1 - \sigma'_3)^2]$

and J_{2o} = is the value of J_2 at the commencement of monotonic loading

J_{2max} = the maximum value of J_2 attainable at the current effective mean stress, p', corresponding to the failure criterion

Pestana and Whittle (1995) proposed a new model for the bulk modulus of sand, which dealt with elastic and elasto-plastic soil behaviour, over a much wider range of stresses than previously considered. The upper limit of mean stress was chosen as the level at which the soil compressibility reached the level of compressibility of the soil water. The model was restricted to either hydrostatic or one-dimensional compression.

The soil compression behaviour upon first loading was considered to consist of elastic compression of the soil matrix and re-arrangement of the particles. At higher stresses, particle breakage occurs and a unique limiting compression curve (LCC) is reached for the soil, regardless of the soil's initial density. The deformation of sand is generally non-linear over the full stress range.

The tangent bulk modulus for elastic response, K_e, was given by:

$$K_e = \frac{C_b}{n} p_a \left(\frac{p'}{p_a}\right)^{1/3} \qquad 3\text{-}20$$

where C_b = a soil constant

n = soil porosity

p_a = atmospheric pressure

The exponent of a third on the mean stress term had a semi-empirical basis.

The full elasto-plastic tangent bulk modulus, K, depended upon four parameters, which included C_b in the above expression. Two of the parameters were associated with the LCC for the soil. The formulation that was given for K was:

$$K = \frac{p_a}{n}\left[\frac{\delta_b^{\theta}}{C_b\left(p'/p_a\right)^{1/3}} + \frac{\lambda_{LCC}\left(1-\delta_b^{\theta}\right)}{\left(p'/p_a\right)}\right] \qquad 3\text{-}21$$

where λ_{LCC} = slope of the LCC in log e - log p′ space

δ_b = a simple function of λ_{LCC} and the reference stress, p'_r

p'_r = effective mean stress on the LCC at a void ratio of 1

θ = an exponent

Typical values of the four material constants were tabulated by Pestana and Whittle and the variations of both p'_r and θ with soil properties were plotted for a range of materials. These plots have been reproduced in Figure 3-4. In the Figure, Ot_u and Ot_g represent Ottawa sand, uniform and graded, respectively. The exponent, θ, expresses the elasto-plastic behaviour of the soil. The higher the value of θ, the more gradual is the change from elastic compression to the LCC. θ is a function of soil grading as expressed by the uniformity coefficient of the soil, C_u, as well as the shape of the particles.

The slope of the LCC was found to be controlled also by particle shape, while the reference stress depended largely on the mean particle size. Soil angularity also affects the reference stress.

Compression of sand under hydrostatic conditions as against one-dimensional compression, affects the position of the LCC, but not its slope. So, the influence of the different stress path could be captured by a change in only one of the four parameters, the reference stress. No guidance was given for other stress paths.

3.3 FRICTION AND DILATION OF SAND

Sand is a frictional material with a coefficient of friction, $\tan\phi'$, where ϕ' is defined as the angle of friction. The friction angle is not a constant for a particular sand, but varies with the levels of stress and strain as well as the degree of packing of the soil.

Rowe (1962) recognized four characteristic values of the friction angle for sand prepared at a single initial value of dry density; ϕ'_{max}, ϕ'_{cv}, ϕ'_{μ} and ϕ'_{f}. The maximum, or peak angle of friction, ϕ'_{max}, was associated with particle packing and aggregate interlock, which is a function of particle shape, particle size and distribution, and soil density. At levels of strain considerably above that needed to reach peak strength, shearing continues without change of volume, at which point, ϕ'_{cv} (or ϕ'_{cs}) is applicable. This parameter represents the critical state strength, which, in the definition of Roscoe, Schofield and Wroth (1958), as reported by Wroth and Bassett (1965), occurs for an isotropic soil when further shear strain is unable to produce changes in effective stress, shear stress or void ratio.

Loose sand behaves differently to dense sand. Dense sand, in a conventional triaxial test, in which a constant confining pressure is applied while the axial pressure is increased, will produce a load/deflection response with a yield, then hardening to a peak strength, followed by softening to the critical state. Loose sand, on the other hand, may not display a distinct peak strength, and the peak friction angle may coincide with the critical state friction angle, ϕ'_{cv}.

Generally, drained triaxial tests on dense sand have been used to define the critical state for sand. The tendency for shear banding can make the interpretation of the tests

difficult and so Been, Jefferies and Hachey (1991) have argued for the use of undrained triaxial tests on loose sand.

Rowe, and many other geotechnical engineers since, regarded ϕ'_{cv} as a soil constant. Been *et al*. (1991) provided evidence (tests on Erksak sand) that the critical state friction angle varied with the void ratio at critical state, tending to lower values as the void ratio increased. From their data it would seem that the assumption of a constant friction angle would not be of any consequence, except for sand at very high void ratios, corresponding to density indices of 10% or less.

Rowe defined the third friction angle, ϕ'_{μ}, as "the true angle of friction of the sand mineral". For quartz sands it was found that ϕ'_{μ} varied with the size of the particles, ranging from 31° for silt-sized particles to 22° for pebbles. Special direct shear tests were employed to evaluate the true friction angle. Both ϕ'_{cv}, and ϕ'_{μ} are regarded as material constants, both independent of packing density.

From consideration of conservation of energy of assemblages of regular particles (balls and spheres), Rowe postulated that ϕ'_{μ} represented the ultimate frictional resistance of the material. His experiments on real soils suggested that a friction angle, $\phi'_{f,}$ was more applicable, which had values intermediate between ϕ'_{cv} and ϕ'_{μ}. In 1972, Rowe considered the sliding actions of irregular shaped particles in confined conditions and concluded that sliding could occur at a number of directions deviating from the mean shear direction. Consequently he defined ϕ'_{f} as the "equivalent angle of friction between particles, modified to include for simultaneous deviations of individual particle directions from the mean direction".

Rowe (1972) proposed that dense sand could initially form groups of locked particles, if the particles were free to move in the plane of the minor principal stresses. Each group of particles could slide against another group until the peak stress was reached and the locked groups were broken. For this situation, ϕ'_{f} approaches the minimum possible value, ϕ'_{μ}. If group action does not occur, he suggested that the sliding surfaces of individual irregular particles are numerous and unpredictable, and the average sliding surface provides a greater frictional resistance

than is represented by ϕ'_{μ}. In such a situation, ϕ'_{f} approaches its maximum value, which is ϕ'_{cv}. In short, Rowe proposed that the maximum value of ϕ'_{f} is attained when "all possible contacts are sliding", while the minimum value is reached "when only a few particle contacts are sliding".

Figure 3-5 from Rowe (1962) depicts the relationship between the four friction angles for a medium-fine sand tested in triaxial compression. In this diagram, ϕ (or ϕ') is plotted against the initial porosity of the sample, n. As the density of the sand increases or the porosity decreases, the peak friction angle increases above ϕ'_{cv} (slightly less than 32° for the sand). The friction angle, ϕ'_{f}, decreases as ϕ'_{max} increases. At the minimum porosity or most dense state, ϕ'_{f}, is approximated by ϕ'_{μ} (26° for this sand).

It has long been understood that the strength of sands is affected by the tendency of the material to dilate or increase volume when sheared. According to Rowe (1962), the phenomenon of dilatancy was recognised by Reynolds in 1885.

Primarily, dilatancy is a function of particle shape, particle size distribution and packing density. In Figure 3-5, the relationship between dilatancy and the available shear strength is suggested for the sand at a chosen initial porosity. The difference between ϕ'_{max} and ϕ'_{f} is attributed to the energy spent on dilation. The difference between ϕ'_{f} and ϕ'_{μ} is attributed to the energy spent on rearranging the particle packing, while friction is solely responsible for ϕ'_{μ}.

The points represented by the clear circles in Figure 3-5 represent values of ϕ'_{f} derived from Rowe's theoretical equation between stress, strain and the friction angle, the equation being more commonly referred to as Rowe's stress-dilatancy expression. His expression is:

$$\frac{\sigma'_1}{\sigma'_3}\left(1-\mathrm{d}\varepsilon_v \Big/ \mathrm{d}\varepsilon_1\right)^{-1} = \tan^2(45^\circ + \frac{1}{2}\phi'_f) \qquad 3\text{-}22$$

or

$$\frac{R}{D_R} = K \qquad 3\text{-}23$$

where $R = \frac{\sigma_1'}{\sigma_3'}$ = principal stress ratio

$D_R = \left(1 - d\varepsilon_v / d\varepsilon_1\right)$

= Rowe's dilatancy rate, where $d\varepsilon_v$ is the total volumetric strain increment and $d\varepsilon_1$ is the major principal total strain increment[1]

$K = \tan^2(45^\circ - \frac{1}{2}\phi_f')$ = ratio of "work in" to "work out"

From these equations, it is clear that a plot of R against D_R will reveal the friction angle, ϕ'_f.

As Rowe indicated in Figure 3-5, the available peak strength in a dilational material (ϕ_{max}) is equal to the ultimate frictional resistance (ϕ_f), plus an increment which depends on the dilatancy rate, D_R.

Bolton (1986) reviewed available data on shear strength of sands tested under both plane strain and triaxial conditions. He adopted a dilation rate, D_B, similar to Rowe's, based on total strains (sum of plastic and elastic components):

$$D_B = -\frac{d\varepsilon_v}{d\varepsilon_1} \qquad 3\text{-}24$$

Again there was no separation of plastic strain from total strain. In plane strain, a dilation angle, Ψ, may be defined by the expression:

$$\sin\Psi = -\frac{d\varepsilon_v}{d\gamma} \qquad 3\text{-}25$$

where $d\gamma$ = engineering shear strain increment = $(d\varepsilon_1 - d\varepsilon_3)$,

[1] Rowe's original equation was based on inconsistent signs for principal and volumetric strains and so the negative sign was replaced by a positive sign

and $d\varepsilon_3$ = increment of minor principal strain.

Bolton recognized that the dilation angle was difficult to define for triaxial conditions.

A further parameter was introduced by Bolton, the relative dilatancy index, I_R. This index incorporated the density index or relative density of the sand, I_D, and a mean stress ratio, $\frac{p'_{crit}}{p'}$, with p'_{crit} being the effective mean stress at which dilation is suppressed by initiation of grain crushing. A value of the critical mean stress of 22 MPa was found to be adequate for the rounded quartz sands in the study, leading to the expression for the dilatancy index:

$$I_R = I_D(Q - \ln p') - R \qquad 3\text{-}26$$

where, Q and R are material constants, which had recommended values of 10 and 1, respectively, for rounded quartz sands.

Bolton warned that the value of 10 in the equation may need to be reduced for weaker grained sands. Ajalloeian and Yu (1996) however reported a value greater than 10 (11.7) for Stockton beach sand, a quartz sand from Newcastle in NSW.

Bolton's investigation of the variation of the maximum dilation rate and dilation angle measured at q/p'_{max}, and the dilatancy index, led to the following proposals for rounded quartz sands having I_R less than or equal to 4:

Plane strain or triaxial: $D_{Bmax} = 0.3I_R$ (where I_R is in radians) 3-27

Triaxial: $(\phi'_{max} - \phi'_{cv}) = 3I_R°$ (where I_R is in degrees) 3-28

Plane strain: $(\phi'_{max} - \phi'_{cv}) = 5I_R° = 0.8\Psi$ (where I_R is in degrees) 3-29

As pointed out by Bolton, the simple saw tooth model of dilatancy in plane strain leads to a higher dilation angle, i.e.:

$$(\phi'_{max} - \phi'_{cv}) = \Psi \qquad 3\text{-}30$$

It is not clear in Bolton's paper if the density index at the start of the test, rather than the density index at the peak strength, was used in the correlations between dilation and dilatancy index, I_R. Presumably it was the former given the practical approach taken by the author. The mean effective stress in the formulation for I_R was the value at failure of the soil.

Bolton's empirical equations conveniently relate maximum dilation rate to density index and mean stress. When the density index of the soil is low, little dilation will be realised. If the effective mean stress is high, dilation will be suppressed. For example, a sand compacted to a density index of 50%, requires an effective mean stress of almost 3 MPa to suppress dilation.

3.4 YIELD SURFACES

A yield surface indicates the combination of stresses that must not be exceeded in order to avoid further yielding or plastic deformation of the soil. As suggested by Lade (1997), a yield surface or yield locus can be considered to be also a contour of constant plastic work. A new yield surface is produced if the plastic deformation is increased. Therefore new yield surfaces are generated as the maximum mean stress, p_o', experienced by the soil is increased.

The intrinsic shape of yield surfaces is usually assumed to be fixed for a soil (Wood 1990). For saturated clay soils, the modified Cam-clay model (Roscoe and Burland 1968) imposes elliptical shapes for the yield loci in q-p′ space. Each ellipse emanates from the origin of the q-p′ plot. Skewed ellipses have been postulated for sands, as will be discussed later.

An example of a set of yield surfaces is provided in Figure 3-6. To progress from one yield surface to the next, the soil must be loaded above the the current value of p_o', say from p_{o1}' to p_{o2}'. The stresses imposed upon the soil must take the soil further down the isotropic normal compression line (or ICL), to cause irreversible or plastic deformation of the soil (refer Figure 3-7 for typical plots of specific volume, v, against effective mean stress, p′, or natural logarithm of p′). Not all the soil deformation is irreversible. When the soil is unloaded and re-loaded, it follows the path of the "url" or unloading-rebound line, which is assumed to represent purely elastic behaviour.

If the soil is initially at $p_{o1}'$and stresses are applied to take the soil along the ICL, for example from A to B in Figure 3-7, the yield surface will change. The vertical distance, AA_1, between the two url's emanating from A and B, represents the plastic deformation experienced by the soil in reaching point B. The vertical distance, A_1A_2, represents the portion of the total soil deformation that may be recovered by unloading the soil from p_{o2}' to p_{o1}', i.e. the elastic deformation. So it can be seen that plastic strains occur when the size of the yield locus is increased.

The soil does not have to be isotropically normally consolidated for it to experience a change in yield surface. An overconsolidated soil is represented by a point on a url away from its intersection with the ICL, for example point J on url 1 in Figure 3-7. An increase of stress may take the soil to point K on url 2, thereby changing the yield surface. If the linear equations for the url's and the ICL for the soil are known for the plot of specific volume against natural logarithm of effective mean stress, it is a simple matter to proportion the plastic and elastic components of deformation for the path JK. In particular, the plastic volumetric strain is given by:

$$\frac{\delta v^p}{v} = \delta\varepsilon_p^p = (\lambda - \kappa)\frac{\delta p_o'}{v p_o'} \qquad 3\text{-}31$$

where λ and κ are the gradients of the ICL and url respectively.

Various stress paths can be taken to expand the yield surface. The stress path, CD, indicated in Figure 3-6 may represent one-dimensional compression. A vertical excursion from A would represent a constant mean stress triaxial test. Referring to Figure 3-7, a constant mean stress test would follow the path AA_1, and create only plastic volumetric strains. Triaxial tests can also be conducted which prevent changes of volume of the specimen, termed a constant volume test. An initial cell pressure is selected, and the deviator stress is slowly increased. As volume strains are sensed by the monitoring system, the cell pressure is adjusted (usually decreased, causing a reduction in mean stress) until the volume change is negated. Although the total volume of the soil remains the same, plastic and elastic deformations develop, which must be of equal magnitude and of opposite sign.

3.4.1 Empirical Yield Surfaces for Sands

Yield loci may be expressed by the function $f(p', q, p'_o)$. Loci may be established by determining the yield points for a series of tests on soil pre-consolidated to p'_o. From this common starting point of stress, various stress paths may be taken to explore the yield surfaces or loci. The yield point is determined from the stress-strain plot for each stress path and segments of yield surfaces are constructed by joining the yield points plotted in q-p′ space.

Poorooshasb, Holubec and Sherbourne (1967) determined the shape of yield surfaces for Ottawa sand in triaxial compression with stress path probing. Yield surfaces appeared to be approximated by straight lines described by the equation:

$$f = c\sqrt{2}(\eta) \qquad 3\text{-}32$$

where η = stress ratio

$$= \frac{q}{p'}$$

and c = close to but less than unity

The coefficient, c, was deemed to be a function of stress state and void ratio.

Tatsuoka and Ishihara (1974) performed similar experiments on Fuji River sand, but found the yield surface segments indicated significantly curved loci, which could be expressed by the equation:

$$\eta = F(p') + \eta_o \qquad 3\text{-}33$$

where $\eta_o = \eta$ for the chosen reference mean stress, p'_o

and $F(p')$ = an empirically derived function, varying from 0 to –1 as p' varies from 1 to 10 kg/cm^2 (Note: 1 kg/cm^2 is equivalent to 98.1 kPa).

Yield curves for Fuji River sand are provided in Figure 3-8, along with the function, $F(p')$, which can be seen to vary with void ratio (or density index), as well as effective mean stress. The yield surface segments have been overlain by continuous curves, which were generated by equation 3-33.

Miura, Murata and Yasufuku (1984) tested Toyoura sand in both compression and tension. Yield surface segments are shown in Figure 3-9, both the broken lines and solid lines in this Figure distinguish different methods of determining the yield point. Again the yield surfaces appear to be distinctively curved especially at high levels of effective mean stress (above 11 MPa).

Wroth and Houlsby (1985) attributed the curved yield surfaces for sands at high stress levels to particle crushing and they suggested that a linear yield locus may be a reasonable approximation for hard grained soils at low levels of stress. Crushing of sand particles of Erksak sand has been reported at an effective mean stress of 1 MPa by Jeffries, Been and Hachey (1991). Coop and Lee (1993) found that a similar level of p' was appropriate for the initiation of particle breakage of Ham River sand, while stress levels of around only 100 kPa were sufficient to cause crushing of Dogs Bay sand. The latter sand was a carbonate-rich sand.

3.5 PLASTIC POTENTIALS AND FLOW RULES

Yielding produces plastic strains which may be considered to be comprised of volumetric and shear components, ε_p^p and ε_q^p, respectively. If the components of the plastic deformation are known for an increment of total strain, $\delta\varepsilon$, a plastic strain vector may be created in a plot of ε_q^p against ε_p^p. Usually this is achieved by subtracting the elastic components from the total volumetric and deviatoric strains.

It is convenient to superimpose the plastic strain vector on a plot of q against p′. The strain vector is initiated from the stress components, which define the yield stresses for the soil. A series of strain vectors at different stress states may be established and small lines drawn normal to the vectors, through the origin of the vectors, tend to form a series of curves of similar shape. These curves are termed "plastic potentials" and may be described by the function, g (p′, q, Π), where Π is a proportionality factor.

It follows then that the increments of plastic strain are related to the plastic potential through differentiation of the plastic potential function as follows;

$$\delta\varepsilon_p^p = \Pi\frac{\partial g}{\partial p'} \quad \text{and} \quad \delta\varepsilon_q^p = \Pi\frac{\partial g}{\partial q} \qquad 3\text{-}34$$

or,
$$D = \frac{\delta\varepsilon_p^p}{\delta\varepsilon_q^p} = \frac{\partial g}{\partial p'}\frac{\partial q}{\partial g} \qquad 3\text{-}35$$

where D represents the plastic dilation of the soil. The last equation is termed a flow rule as it relates the relative increase of plastic strain components with the state of stress.

Conversely, the plastic potential function may be derived from knowledge of the dilation of the soil material.

When the shape of the plastic potentials are identical with the shape of the yield loci, the soil is said to be associative, or it may be stated that the soil follows the associated flow rule.

Since; $$f = g \qquad 3\text{-}36$$

then, $$D = \frac{\delta\varepsilon_p^p}{\delta\varepsilon_q^p} = \frac{\partial f}{\partial p'}\frac{\partial q}{\partial f} \qquad 3\text{-}37$$

If the shape of the yield locus is known, the components of the plastic deformation of an associative soil can be determined from the stress components.

Reconstituted clays are often considered to be associative and the modified Cam-clay model assumes that an associated flow rule applies. Assuming the yield loci in Figure 3-6 represent modified Cam-clay, the critical state line must pass through the apex of each ellipse, since the soil at critical state, by definition, undergoes unlimited plastic shear strain with no change in volume. Therefore the incremental plastic strain vector must pass vertically through the apex.

However, there is significant evidence to suggest sands are non-associative, e.g., Coop, 1993 (Ham River sand) and Anandarajah, Sobhan and Kuganenthira, 1995 (Ottawa sand). The tests on Toyoura sand by Miura, *et al*. (1984), were interpreted by the researchers to give segments of plastic potentials. A copy of the plotted potentials is provided in Figure 3-10. The shapes of the plastic potentials do not match the shapes of the yield loci in the companion Figure 3-9.

The earlier research by Poorooshasb, et al (1966) demonstrated that Ottawa sand was also non-associative, as is evident in Figure 3-11 for medium dense to very dense sand. The plots essentially are q-p′ plots, although other definitions of stress were applied by these authors (see note to Figure). The plastic potentials are almost elliptical while the yield loci for the stress range (p′ <1.5 MPa) approximated straight lines at constant stress ratio through the origin.

3.5.1 Flow Rules

The modified Cam-clay flow rule for associative soils takes the form (Wood 1990);

$$D = \frac{M_c^2 - \eta^2}{2\eta} \qquad 3\text{-}38$$

where $M_c = \frac{q}{p'}$ at the critical state

and η is the current value of $\frac{q}{p'}$.

Davis (1969) proposed a non-associative flow rule for frictional soil under a state of plane strain loading, relating the rate of plastic strain to the dilation angle, ψ:

$$\frac{d\varepsilon_3^p}{d\varepsilon_1^p} = \tan^2(45 + \psi/2) = -N_\psi \qquad 3\text{-}39$$

The Davis flow rule was extended to triaxial compression by Carter, Booker and Yeung (1986).

$$\frac{d\varepsilon_1^p}{2d\varepsilon_3^p} = \frac{1}{\tan^2(45 + \psi/2)} = -\frac{1}{N_\psi} \qquad 3\text{-}40$$

In this case the dilation rate, D, may be expressed by:

$$D = \frac{-6\sin\Psi}{(3 - \sin\Psi)} = -M_\psi \qquad 3\text{-}41$$

The term M_ψ is of a similar form to M, which is a function of ϕ'.

The most commonly accepted flow rule for sand is based on Rowe's (1962) expression between stress and rate of dilatancy. Wood (1990) integrated Rowe's equation to derive the plastic potential and so derived the following flow rule:

$$D = \frac{9(M_c - \eta)}{(9 + 3M_c - 2M_c\eta)} \qquad 3\text{-}42$$

Like the Modified Cam-clay flow rule, dilatancy is reduced as the stress state of the soil approaches the critical state.

The flow rule given in equation 3-42 is applicable to triaxial conditions and, as pointed out by Wood, is appropriate where sliding of particles occurs, i.e. when the soil is sheared and not when it is undergoing isotropic compression. Inherent in this flow rule are the assumptions that elastic strains are negligible, since Rowe worked with total strains, and secondly, that the ultimate frictional resistance of the sand, ϕ'_f, can be approximated by the critical state value, ϕ'_{cv} (the upper limit of its value). The latter assumption may lead to underestimation of the contribution of dilation to the strength of dense sand. Referring to Figure 3-5, ϕ'_{cv} is increasingly less than ϕ'_f, with increasing sand density (or decreasing sand porosity).

Generally this flow rule has been thought to be too cumbersome to employ in numerical models, and so approximations have been sought, for example, Wood, Belkheir and Liu (1994) proposed:

$$D = A(M_c - \eta) \qquad 3\text{-}43$$

where A = a constant

Although guidance on values of A was not given, examples within the paper suggested values between one and two were applicable. A value of one produces the original Cam clay flow rule. Comparing the two flow rules for sands yields an expression for A:

$$A = \frac{9}{(9 + 3M_c - 2M_c\eta)} \qquad 3\text{-}44$$

The flow rules in this section can be represented by plots of η against β, the dilatancy angle, defined by Wood (1990) as:

$$\beta = a\tan(\frac{1}{D}) = a\tan\left(\frac{\delta\varepsilon_q^p}{\delta\varepsilon_p^p}\right) \qquad 3\text{-}45$$

Figure 3-12 contains two plots of η against β, for two values of ϕ'_{cv}, 31° and 27°. All four flow rules impose a value of β of 90° when η equals M_c. In other words, the plastic volumetric strain increment and dilation, D, are zero once critical state is reached, as required by critical state theory. Modified Cam clay implies greater dilation at low stress ratios than any other of the flow rules.

The major difference between the flow rules is evident at η equal to zero, representing isotropic compression. The modified Cam clay model forces β to zero, thereby eliminating any plastic shear strain increments when η is zero. The other flow rules enforce a value of β of approximately 45°, suggesting nearly equal increments of both plastic volumetric and plastic shear strains under isotropic compression. Plastic shear strain increments have been recorded for sands at low stress ratios as demonstrated in Figure 3-11, which was taken from Poorooshasb, et al 1966. However the dilatancy angle at η equal to zero in this Figure (i.e. at points on the horizontal axis) does not appear to be greater than 30°, generally.

The flow rule of Wood, Belkheir and Liu (1994) was initially implemented with a value of their parameter, A, of two. However it was soon realised that the correspondence the authors wished to achieve with Rowe's flow rule could only be achieved if a value of about 0.75 was adopted. It appears that A should vary between 0.5 and 1, not 1 and 2.

Manzari and Dafalias (1997) related dilation to the stress ratio at the onset of dilation, M_c^d. Figure 3-13 provides a visual definition of M_c^d for a constant p′ triaxial test. In the top diagram, the excursion in e - lnp′ space is illustrated with the soil consolidating between points 1 and 2, with point 2 representing the onset of dilation. As dilation proceeds, the soil reaches peak strength (point 3, which can not be shown) and eventually softens to the critical state (point 4). The same stress excursion is illustrated in the lower Figure in q-p′ space, but with both axes

normalized with respect to p′. The stress ratio, η = q/p′, traverses from M_c^d, M and finally to M_c between points 2, 3 and 4, which correspond to the same points in the top Figure.

Restricting the discussion to compression only, the flow rule proposed by Manzari and Dafalias was:

$$D = \sqrt{\frac{2}{3}}\left(A\left(M_c^d - \eta\right)\right) \qquad 3\text{-}46$$

The stress ratio, M_c^d, is not a soil constant. The difference between M_c, the critical state stress ratio, and M_c^d, was expressed as a function of the difference in void ratios, e, the current void ratio at effective mean stress, p′, and the critical state void ratio for the same level of mean stress, i.e.:

$$\left(M_c - M_c^d\right) \propto \left(e - e_c\right) \qquad 3\text{-}47$$

As the void ratio, e, tends towards e_c, M_c^d tends towards M_c. Dilation can not occur once the soil reaches its critical state (provided also that the current stress ratio is less than M_c^d). The term on the right hand side of equation 3-47 is now known as the "state parameter", which is discussed in the next section.

3.6 STATE PARAMETER

Poorooshasb et al (1966) discussed the importance of "state" on the behaviour of sand. In their definition, "state" described the current void ratio and level of stress of the sand.

In 1985, Been and Jefferies coined the term "state parameter" for sands. The parameter is merely the difference between the current void ratio of the sand and the

void ratio at critical state[2], at the same value of mean stress. Therefore the state parameter largely incorporates the features of "state" required by Poorooshasb *et al.* (1966). Although Been and Jefferies promoted the use of state parameter to assist in understanding the behaviour of sand, they pointed out that soil fabric was also an important consideration.

State parameter, ξ, may be expressed as:

$$\xi = e - e_c \qquad 3\text{-}48$$

where e = current void ratio for soil at an effective mean stress of p'

and e_c = void ratio at critical state and at p'

Since the critical state line or CSL for a sand may be approximated by a straight line in a plot of void ratio against the natural logarithm of effective mean stress, it follows that the state parameter may be defined as:

$$\xi = e - \Gamma + \lambda_{ss} \ln p' \qquad 3\text{-}49$$

where $\Gamma = e_c$ at a reference mean stress (usually 1 kPa)

and λ_{ss} = the slope of the critical state line (CSL)

The state parameter concept is illustrated in Figure 3-14. Soil may be at an initial effective mean stress of p'_1 and have an initial dry density corresponding to a void ratio of e_1. The void ratio must be substantially increased (to e_{c1}) for the soil to reach critical state at the same mean effective stress level. Therefore substantial dilation must occur. Accordingly the state parameter, ξ_1, is relatively high. However if the mean stress is increased to p'_2, the state parameter decreases to ξ_2, and less dilation is required to reach the critical state.

[2] The term "steady state" of sand was used in preference to "critical state", the definitions of the two states being similar but not identical. In a later paper (Been, Jefferies and Hachey 1991), it was argued that the two states are indistinguishable experimentally and so, in this thesis, only the term critical state has been adopted.

In this illustration, the stress excursion from p'_1 to p'_2 would represent a constant volume test if the void ratio remained constant. It is evident that in a constant volume test, the value of the state parameter is reduced by $\lambda_{ss}\left[\ln\left(p'_2/p'_1\right)\right]$. In summary, for a sand with a negative state parameter, as ξ increases, i.e. as it tends to zero, dilation is less likely.

The critical state line for sand is influenced by impurities in the soil. Hird and Hassona (1986) found that increasing the mica content of Leighton-Buzzard sand increased the magnitudes of both Γ and λ_{ss}. In contrast, Been and Jefferies (1985) reported that increasing the silt content of Kogyuk sand decreased Γ and λ_{ss}.

A number of researchers have tested sand and have subsequently determined the CSL for each particular soil. A summary is provided of both the CSL's defined in the literature and the key properties of the sands, in Tables 3-III and 3-IV, respectively. The various sources of the information are also provided. The different CSL's in Table III have been plotted together in Figure 3-15.

The CSL constants are generally applicable for effective mean stress levels less than 1 MPa. The intercept, Γ, is based on a reference effective mean pressure of 1 kPa, and the gradient, λ, is based on the natural logarithm of the effective mean stress.

At effective mean stresses greater than 1 MPa, some researchers have found that sand can exhibit increased compressibility (larger values of λ), which has been shown to be associated with particle crushing (Been, Jefferies, and Hachey, 1991, Ajalloeian and Yu, 1996, and the work of others reported by Sasitharan *et al*., 1994).

The majority of the sands reported in the literature were rounded to sub-rounded. The variability of the CSL's is quite evident in Figure 3-15. Gradients of the CSL varied between 0.013 to 0.037, while the intercept ranged between 0.75 and 1.05. Averages for the twelve soils were a gradient of 0.023 and an intercept of 0.92. Correlations were sought between the soil properties and the corresponding CSL constants, but no clear trends were evident.

3.6.1 State Parameter and Soil Strength

Been and Jefferies (1985) found that the state parameter correlated well with the difference between peak and critical state friction angles, $\phi' - \phi'_{cv}$ (shown as $\phi' - \phi'_{ss}$ in their Figure). The correlation (reproduced in Figure 3-16) was based on thirteen sands from around the world (Been and Jefferies, 1986). As the critical state friction angle showed little variation, usually ranging between 30 and 32°, the authors also presented a plot of ϕ'_{max} against state parameter, which appeared to be fruitful. Data from a further seven sands was added by Been and Jefferies in 1986, and it is this later plot which is reproduced in Figure 3-17. The data were derived from sub-angular and sub-rounded sands. Limited experience with angular sand produced similar behaviour, but was not consistent with the established upper and lower bounds shown in the plots.

The realisation that the difference between the current available shear strength of sand is related to state parameter, has led other researchers to assume that state parameter is linked to dilation. This assumption flows from the research of Rowe (1962).

Collins, Pender and Yan (1992) interpreted the experimental data of Been and Jefferies 1985 and proposed the following relationship;

$$(\phi' - \phi'_{cv}) = A(e^{-\xi} - 1) \qquad 3\text{-}50$$

The coefficient A has been reported to have values ranging between 0.6 and 0.93 (refer Table III).

This equation may be compared with Bolton's equations (3-28 and 3-29), which relate the difference in friction angle to a dilatancy index rather than state parameter.

3.6.2 Numerical Models Involving State Parameter

A number of authors have implemented state parameter models for sands. It is not the purpose of this section to review these models, rather it is to note their existence.

Manzari and Dafalias (1997) developed a state parameter constitutive model capable of simulating triaxial monotonic and cyclic loading response of sands. A minimum of eight material constants was required for the model.

Yu (1998) attempted to bridge the gap between clays and sands, with the introduction of the constitutive model, CASM. CASM included the state parameter concept for sands.

Islam, Carter and Airey (1999) proposed a state parameter constitutive model specifically for cemented and non-cemented carbonate sands. A feature of these particular sands is the angularity of particles and consequently the relatively high shear strengths the sands can achieve.

3.7 SUMMARY OF THE CHAPTER

It may be concluded that the initial modulus (E_o, G_o or K_o) of sand is a function of the type of sand (in particular, the shape of the particles), the density of the sand and the effective mean stress, which is applied to the soil. The change of modulus with application of shear stress depends upon the level of applied shear stress, relative to the maximum shear stress that can be sustained by the soil.

Young's modulus, E, shear modulus, G, and bulk modulus, K, all vary with stress and, for that matter, also with strain. The relationships between E, G and K are dependent upon Poisson's ratio, which may change with soil density.

It is evident from this literature review that a constitutive model for sand, which defines the pre- and post-yield of the soil, should allow initial non-linear behaviour and incorporate the two key concepts of critical state and the state parameter. In Chapter 5 of this thesis, the behaviour of the sand in terms of non-linear loading response and critical state, and dilation with respect to state parameter, are addressed. The testing program on the sand is presented and results of the testing are analysed.

A constitutive model is then developed in Chapter 6. The constitutive model employs many of the fundamental theories discussed in this Chapter. In this model, the influence of soil fabric was not addressed.

3.8 REFERENCES TO CHAPTER 3

Ajalloeian, R. and Yu, H.S. (1996). A Calibration Chamber Study of Self Boring Pressuremeter Tests in Sand. Proc., 7th ANZ Geomechanics Conference, Adelaide, pp 60-65.

Barnes, G. E. (2000). Soil Mechanics: Principles and Practice. MacMillan Press, 2nd edition.

Been, K. and Jefferies, M.G. (1985). A State Parameter for Sands. Geotechnique, 35, No. 2, pp 99-112.

Been, K. and Jefferies, M.G. (1986). Discussion on "A State Parameter for Sands", by Been and Jefferies (1985). Authors' reply, Geotechnique, 36, No. 1, pp 127-132.

Been, K., Jefferies, M.G., Crooks, J.H.A. and Rothenburg, L. (1987). The Cone Penetration Test in Sands: Part II, General Inference of State. Geotechnique, 37, No. 3, pp 285-299.

Been, K., Jefferies, M.G. and Hachey, J. (1991). The Critical State of Sands. Geotechnique, 41, No. 3, pp 365-381.

Been, K and Jefferies, M. G. (1993). Towards Systematic CPT Interpretation. Proc., Predictive Soil Mechanics, Wroth Memorial Symposium, Oxford, 1992, Telford, pp 44-55.

Bolton, M. D. (1986). The Strength and Dilatancy of Sands. Geotechnique, V36, No. 1, pp 65-78.

Carter, J. P., Booker, J. R. and Yeung, S. K. (1986). Cavity Expansion in Cohesive Frictional Soils. Geotechnique, V36, No. 3, pp 349-358.

Chu, J. and Lo, S.-C. R. (1993). On the Measurement of Critical State Parameters of Dense Granular Soils. ASTM, Geotechnical Testing J. (GTJODJ), V16, No. 1, March, pp 27-35.

Collins, I. F. Pender, M. J. and Yan, W. (1992). Cavity Expansion in Sands under Drained Loading Conditions. Int. J. for Num. and Analytical Methods in Geomechanics, V16, No 1, pp 3-23.

Coop, M. R. (1993). The Behaviour of Granular Soils at Elevated Stresses. In "Predictive Soil Mechanics", Proc. Wroth Memorial Symposium, Oxford, 1992, Telford, pp 101-114.

Dakoulas, P. and Sun, Y. (1992). Fine Ottawa Sand : Experimental Behaviour and Theoretical Predictions. ASCE, J. Geotechnical Engineering, V118, No 12, Dec., pp 1906-1923.

Davis, E. H. (1969). Theories of Plasticity and the Failure of Soil Masses. In "Soil Mechanics, Selected Topics", ed. Lee, I. K., Chapter 6, Butterworths, pp 341-380.

Fahey, M. (1991). Measuring Shear Modulus in Sand with the Self-Boring Pressuremeter. X European Conference on Soil Mechanics and Foundation Engineering, V1, Florence, pp 73-76.

Fahey, M. and Carter, J. P. (1993). A Finite Element Study of the Pressuremeter Test in Sand using a Nonlinear Elastic Plastic Model. Canadian Geotechnical J., V30, pp 348-362.

Holubec, I. (1968). Elastic Behaviour of Cohesionless Soil. Journal of Soil Mechanics and Foundation Design, ASCE, V94, No SM6, Nov., pp 1215-1231.

Ishihara, K. (1993). Liquefaction and Flow Failure during Earthquakes. 33rd Rankine Lecture, Geotechnique, 43, pp349-416.

Islam, M. K., Carter, J. P. and Airey, D. W. (1999). A Constitutive Model for Carbonate Sediments. Proc., 8th ANZ Conference on Geomechanics, V2, Hobart, ed.s Vitharana, N. and Colman, R., Australian Geomechanics Society, pp 2-961 to 2-967.

Janbu, N. (1963). Soil Compressibility as Determined by Oedometer and Triaxial Tests. Proc., V1 European Conf. SMFE, Wiesbaden, pp 19-25.

Kerisel, J. (1963). Necessite de Rapporter les Tassements au Rayon Moyen de la Surface Chargee et les Pressions Appliquees aux Pressions Limites. Proc. of the V1 European Conf. SMFE, Wiesbaden, pp 83-88.

Lade, P. V. and Nelson, R. B. (1987). Modelling the Elastic Behaviour of Granular Materials. Int J. for Num. and Analytical Methods in Geomechanics, V11, 521-542.

Lee, J. and Salgado, R. (2000). Analysis of Calibration Chamber Plate Load Tests. Canadian Geotechnical Journal, V37, pp 14-25.

Manzari, M. T. and Dafalias, Y. F. (1997). A Critical State Two-Surface Plasticity Model for Sands. Geotechnique, 47, No. 2, pp 255-272.

Miura, H., Murata, H. and Yasufuku, N. (1984). Stress–strain Characteristics of Sand in a Particle–crushing Region. Soils and Foundations, V24, No. 1, pp 77-89.

Pestana, J. M. and Whittle, A. J. (1995). Compression Model for Cohesionless Soils. Geotechnique, V45, No. 4, pp 611-631.

Poorooshasb, H. B., Holubec, I. and Sherbourne, A. N. (1966). Yielding and Flow of Sand in Triaxial Compression : Part I. Canadian Geotechnical J., V3, No. 4, November, pp 179-190.

Poorooshasb, H. B., Holubec, I. and Sherbourne, A. N. (1967). Yielding and Flow of Sand in Triaxial Compression : Parts II and III. Canadian Geotechnical J., V4, No. 4, pp 376-397.

Poulos, S. J., Castro, G. and France, J. W. (1985). Liquefaction Evaluation Procedure. J. Geotech. Eng., ASCE, V111, No. 6, June, pp 772-792.

Roscoe and Burland, (1968). On the Generalized Stress Strain Behaviour of Wet Clay. Engineering Plasticity, Cambridge University Press, pp 535-609.

Rowe, P. W. (1962). The Stress-dilatancy Relation for Static Equilibrium of an Assembly of Particles in Contact". Proc. Royal Society, V267, pp 500-527.

Rowe, P. W. (1972). Theoretical Meaning and Observed Values of Deformation Parameters for Soil. Proc., Roscoe Memorial Symposium, "Stress-Strain Behaviour of Soils", Ed. Parry, R. H. G., Cambridge, March, pp 143-194.

Sasitharan, S., Robertson, P. K., Sego, D. C. and Morgenstern, N. R. (1994). State Boundary Surface for Very Loose Sand and its Practical Implications. Canadian Geotech. J., V31, No. 3, pp 321-334.

Schanz, T. and Vermeer, P. A. (1996). Angles of Friction and Dilatancy of Sand. Technical Note, Geotechnique, V46, No. 1, pp 145-151.

Tatsuoka, F.and Ishihara, K. (1974). Yielding of Sand in Triaxial Compression. Soils and Foundations, V14, No. 2, pp 63-76.

Wood, D. M. (1990). Soil Behaviour and Critical State Soil Mechnanics. Cambridge University Press.

Wood, D. M., Belkheir, K. and Liu, D. F. (1994). Strain Softening and State Parameter for Sand Modelling. Technical Note, Geotechnique, V44, No. 2, pp 335-339.

Wroth and Bassett (1965). A Stress-strain Relationship for the Shearing Behaviour of a Sand. Geotechnique, V15, No.1, pp32-56.

Wroth, C. P. and Houlsby, G. T. (1985). Soil Mechanics – Property Characterization and Analysis Procedures. Proc., 11th ISSMFE Conf., San Fransisco, V1, pp 1-56.

Xu, K. J., Liu, M. D. and Carter, J. P. (1999). Explicit Stress-Strain Equations for Geo-Materials. Dept. Civil Engineering, University of Sydney, Res. Rept. R751, October.

Yu, H. S. (1994). State Parameter from Self-Boring Pressuremeter Tests in Sand. J. Geotechnical Engineering, ASCE, V120, No.12, pp 2118-2135.

Yu, H. S., Schnaid, F. and Collins, I. F. (1996). Analysis of Cone Pressuremeter Tests in Sands. J. Geotechnical and Geoenvironmental Engineering, ASCE, 122(8), pp 623-632.

Yu, H. S. (1998). CASM: A Unified Constitutive Model for Clay and Sand. Int. J., Numerical and Analytical Methods in Geomechanics, V22, pp 621-653.

Table 3-I. Coefficients for Santa Monica Sand (Lade and Nelson, 1987) and Ottawa Sand (Dakoulas and Sun, 1992).

Sand	State	Density Index, I_D (%)	M	λ	ν
Santa Monica	Loose	20	600	0.27	0.26
	Dense	90	1270	0.23	0.14
Ottawa	Loose	30	590	0.32	0.2
	Dense	75	860	0.24	0.2

Table 3-II. Coefficients for Estimation of G_o according to Richart *et al.* (1970) [from Yu *et al*. (1994)]

Particle Shape	S	n	e_g
rounded	690	0.5	2.17
angular	323	0.5	2.97

TABLE 3-III. Reported Values of Critical State Lines

Sand	λ	Γ	ϕ'_{cs} (°)	A[#]	Reference
Sydney	0.032	0.967	32.5		Chu and Lo 1995
Stockton	0.0374	0.925	31.1	0.93	Ajalloeian and Yu 1996
Hokksund	0.023	0.934	32	0.80*	Been et al 1987
Ottawa	0.012	0.754	28.5	0.95*	Been et al 1987
Ottawa C109	0.017	0.864	29.8		Sasitharan et al 1994
Monterey No. 0	0.013	0.878	32	0.83*	Been et al 1987
Kogyuk, 350/2	0.029	0.849	35	0.75*	Been and Jefferies 1985
Reid-Bedford	0.028	1.014	32	0.63*	Been et al 1987
Ticino	0.024	0.986	31	0.60*	Been et al 1987
Erksak	*0.0133*	*0.820*	*30.9*		*Been et al 1991*
Toyoura 1	0.013	1.00	31		Been et al 1987
Toyoura 2	0.0283	1.048	30.9		Ishihara 1993[+]

[#] Refer equation 3-48

*As reported by Yu 1994

[+]As reported in Sasitharan et al 1994

TABLE 3-IV. Key Soil Properties

Sand	Description		C_u	D_{10} (mm)	Max. and Min. Void Ratios	
	Particle shape	Other			e_{max}	e_{min}
Sydney		uniformly graded	1.5	-	0.855	0.565
Stockton	subrounded		1.71	0.24	0.779	0.497
Hokksund	subangular	feldspar and some mica	2.0	0.21	0.91	0.55
Ottawa	rounded		1.7	0.35	0.79	0.49
Ottawa C109	rounded to subrounded				0.82	0.50
Monterey No. 0	subrounded	trace of feldspar	1.6	0.25	0.82	0.54
Kogyuk 350/2	subrounded to angular	uniform, medium			0.83	0.47
Reid-Bedford	subangular	some feldspar	1.6	0.16	0.87	0.55
Ticino	subrounded	trace of mica	1.6	0.36	0.89	0.6
Erksak	subrounded	uniformly graded, with 22% feldspar and plagioclase	1.8	0.19	0.753	0.527
Toyoura 1			1.3	0.16	0.87	0.66
Toyoura 2	rounded to subrounded	25% feldspar			0.973	0.635

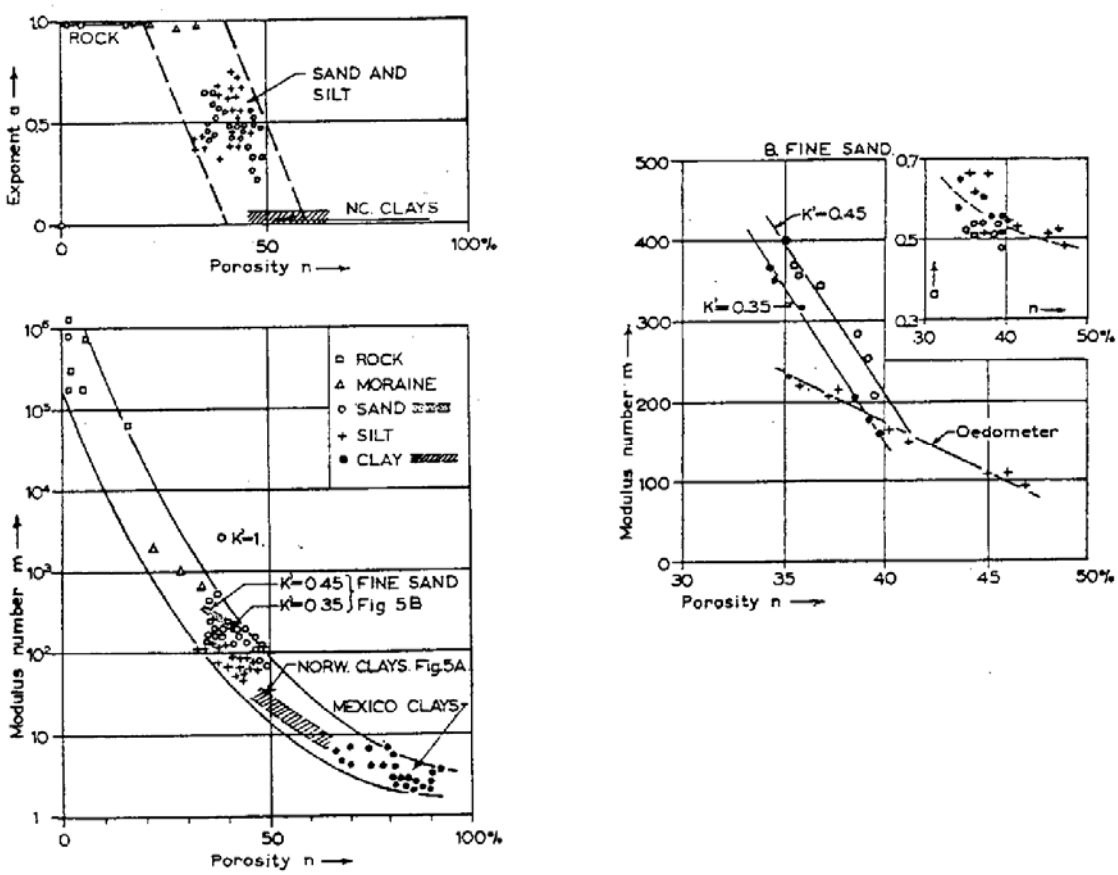

Figure 3-1. The variation of coefficients, a and m, with soil porosity (Janbu, 1963)

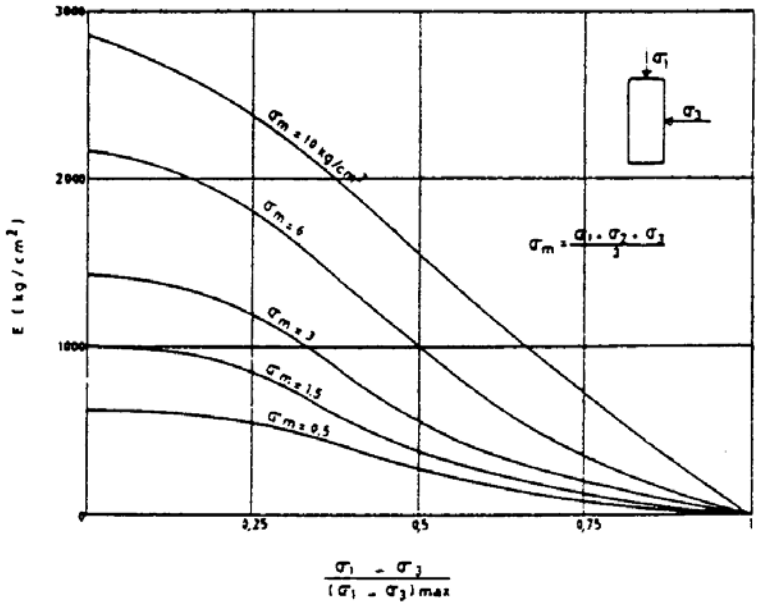

Figure 3-2. Variation of Young's modulus, E, with q /q_f and p (or σ_m) (Kerisel, 1963)

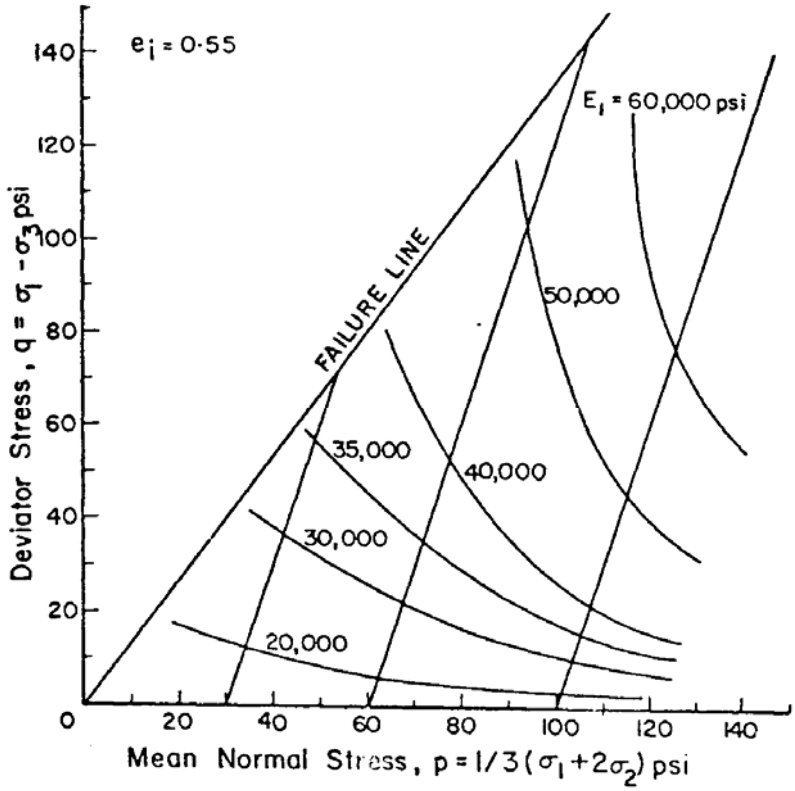

Figure 3-3. Variation of modulus, E_1, of Ottawa sand (initial void ratio = 0.55) with q and p (Holubec , 1968). <u>Note:</u> 1 psi = 6.9 kPa

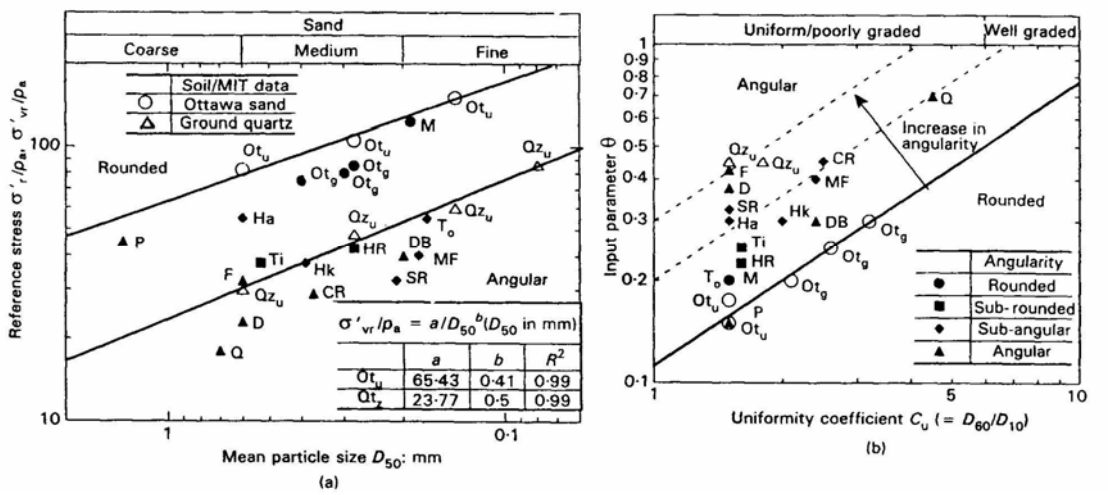

Figure 3-4. Dependence of parameters, p'_r (or σ'_r on Figure (a)) and θ on particle size, shape and distribution (after Pestana and Whittle 1995)

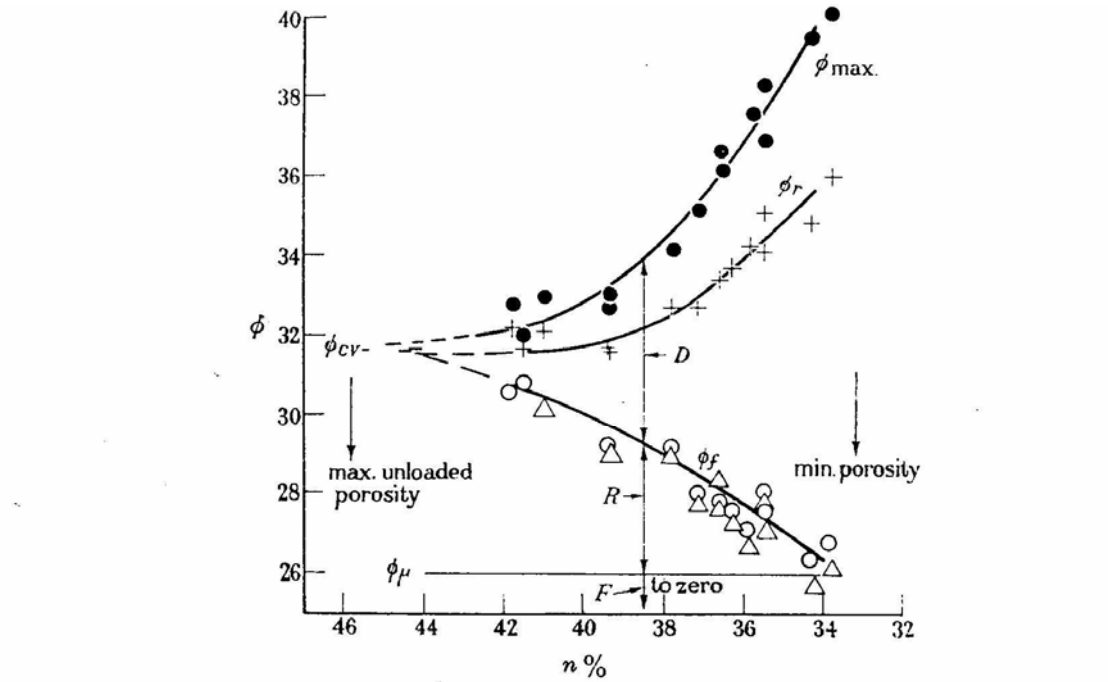

FIGURE 22. Medium-fine sand; over-consolidated to 60 Lb./in.²; tested at $\sigma_3 = 30$ Lb./in.²; rate = 0·0033 in./min; samples 4 in. diam. ●, $\phi_{max.}$ (equation (2)); +, ϕ_r (equation (4)); △, ϕ_f (equations (5) and (7)); ○, ϕ_f (equation (17)). *D*, difference due to energy spent on dilation; *R*, difference due to energy spent on remoulding; *F*, difference due to energy spent in friction.

Figure 3-5. An example of the definitions of friction angles for a sand (from Rowe 1962). Note: 1 Lb./in^2 ≡ 6. 9 kPa and "D" = D_R

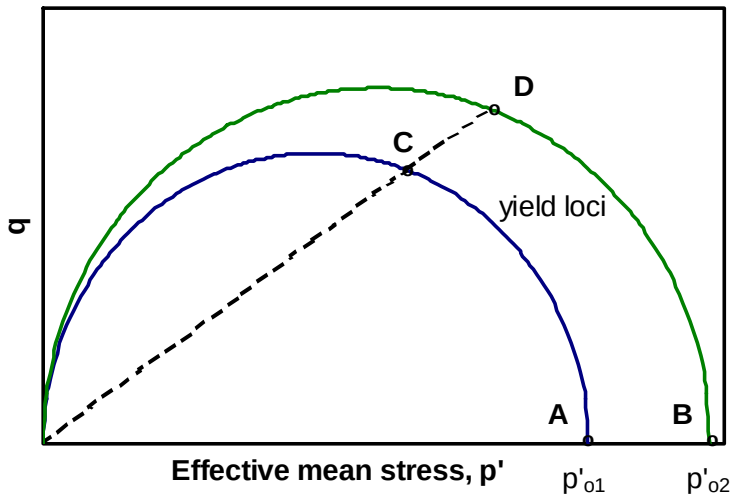

Figure 3-6. Examples of yield surfaces for a saturated clay

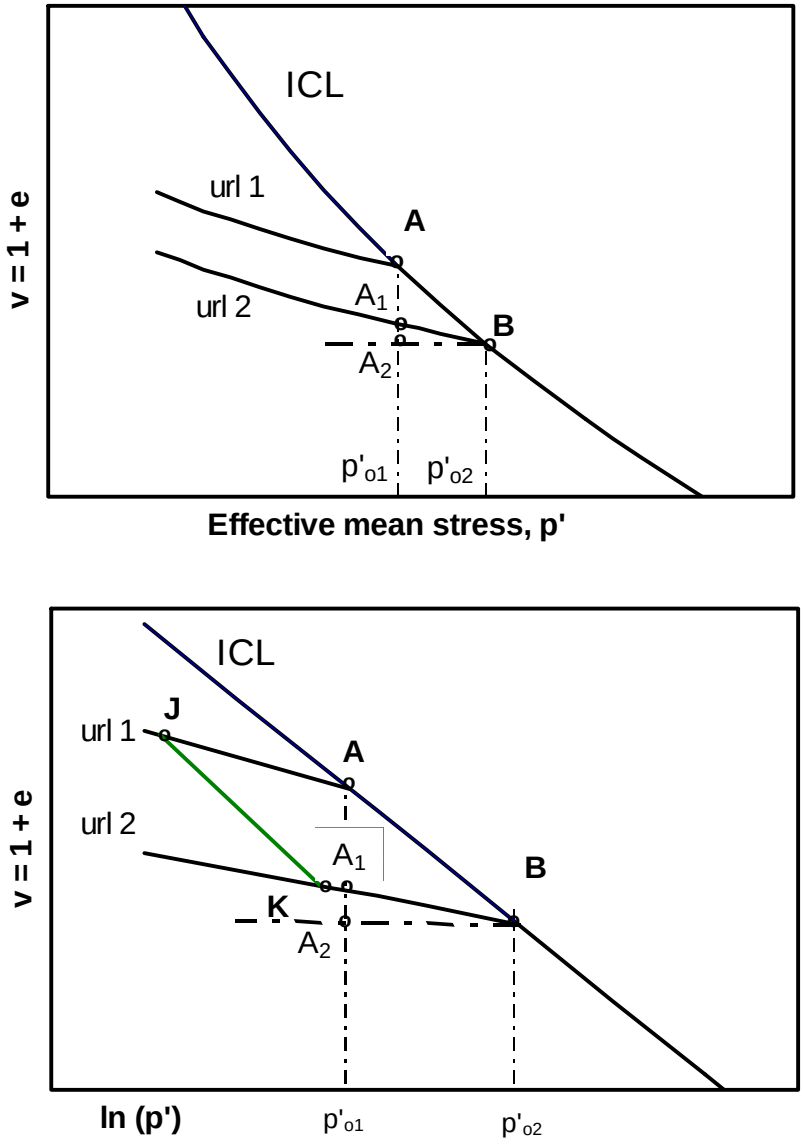

Figure 3-7. Deformations associated with change in yield surface

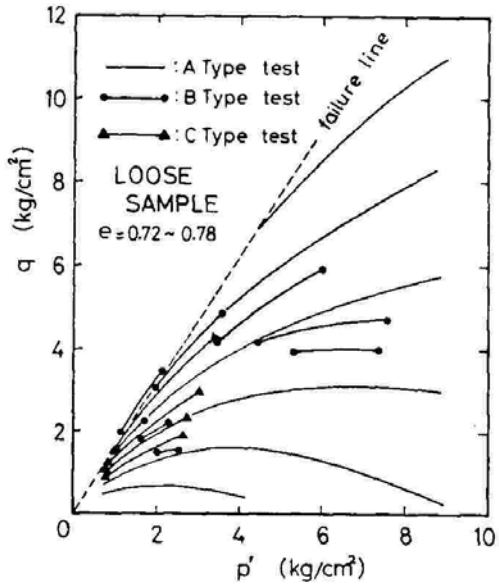

Fig. 12. Yield loci for loose sample

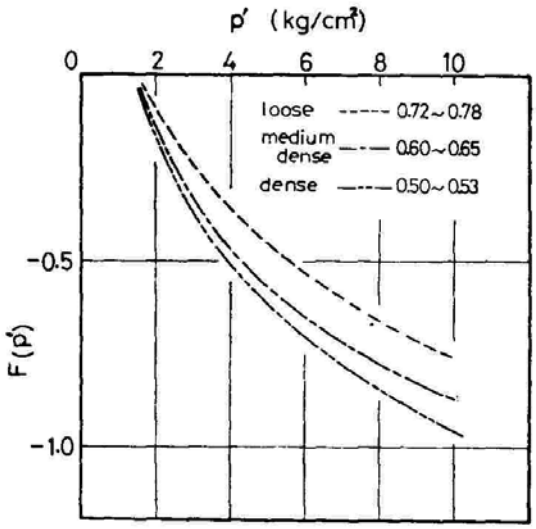

Fig. 13. Dependence of yield characteristics on density

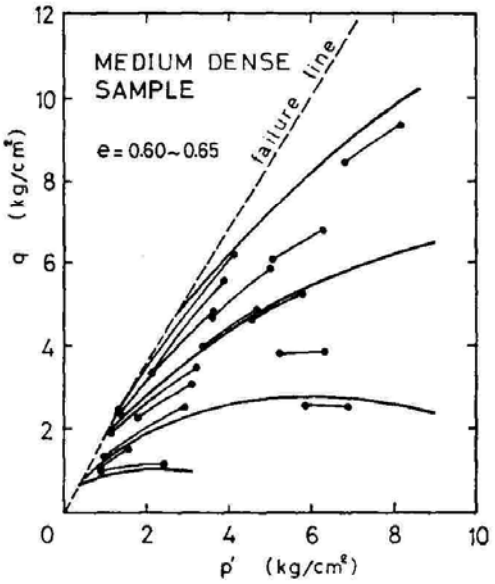

Fig. 14. Yield loci for medium dense sample

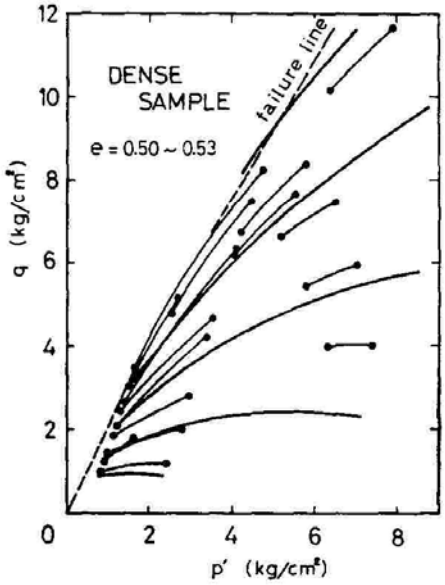

Fig. 15. Yield loci for dense sample

Figure 3-8. Experimental yield surface segments for Fuji River sand (from Tatsuoka and Ishihara 1974). Note: 1 kg/cm^2 is equivalent to 98.1 kPa

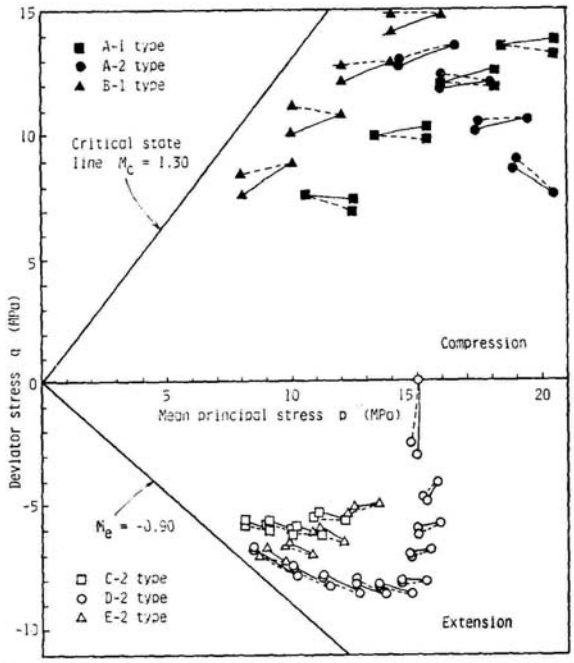

Fig. 6. Family of yield curve segments obtained by triaxial compression and extension tests

Figure 3-9. Yield curve segments for Toyoura sand (from Miura, Murata and Yasufuku, 1984)

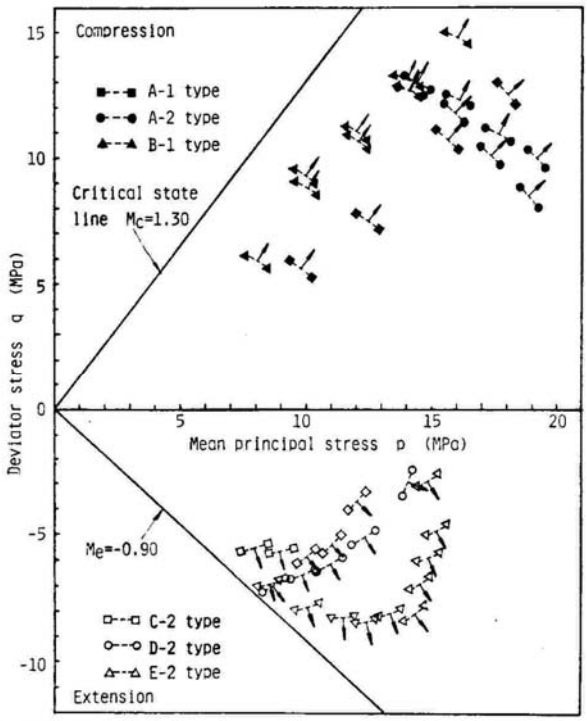

Fig. 8. Family of yield curve segments based on the normality condition

Figure 3-10. Plastic strain vectors and plastic potential segments for Toyoura sand (from Miura, Murata and Yasufuku, 1984)

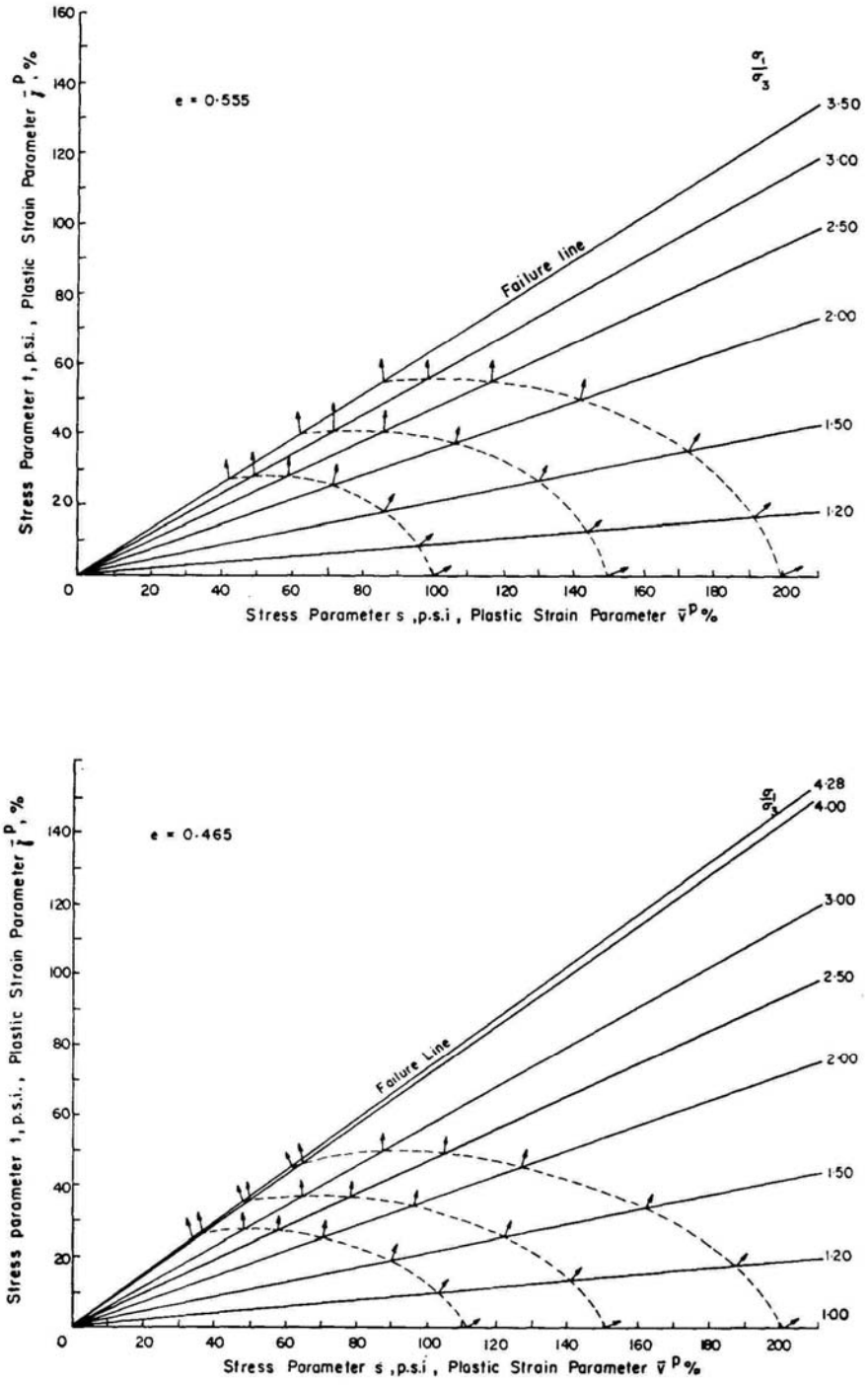

Figure 3-11. Plastic potentials for Ottawa sand prepared at density indices of 70 and 94% or e= 0.555 and e =0.465 (after Poorooshasb, et al 1966).

<u>Notes:</u> 1 psi = 6.9 kPa, s = √3 (p′) and t = √(2/3) (q)

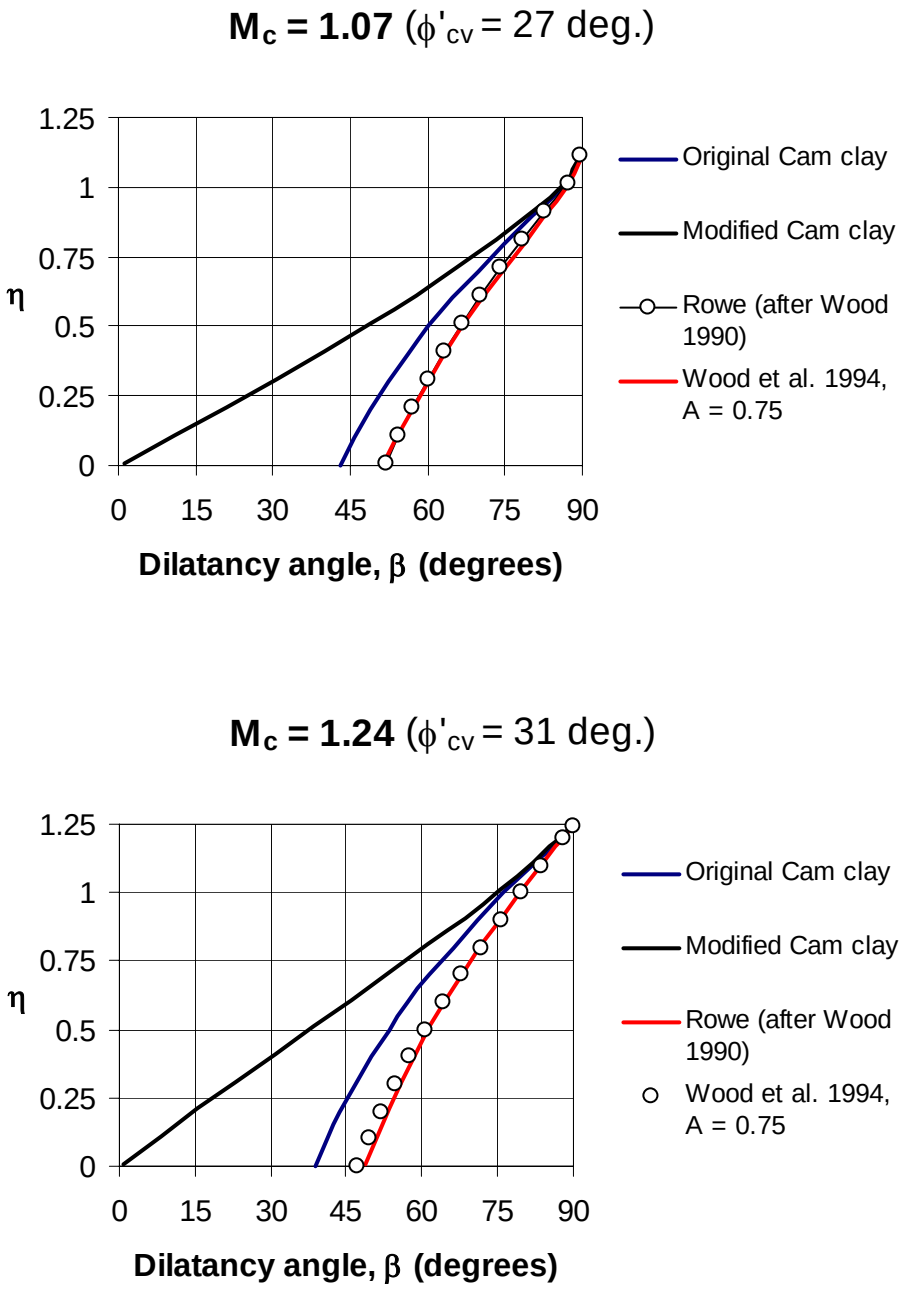

Figure 3-12. Flow rules expressed by the variation of dilatancy angle with stress ratio for ϕ'_{cv} values of 27° and 31°

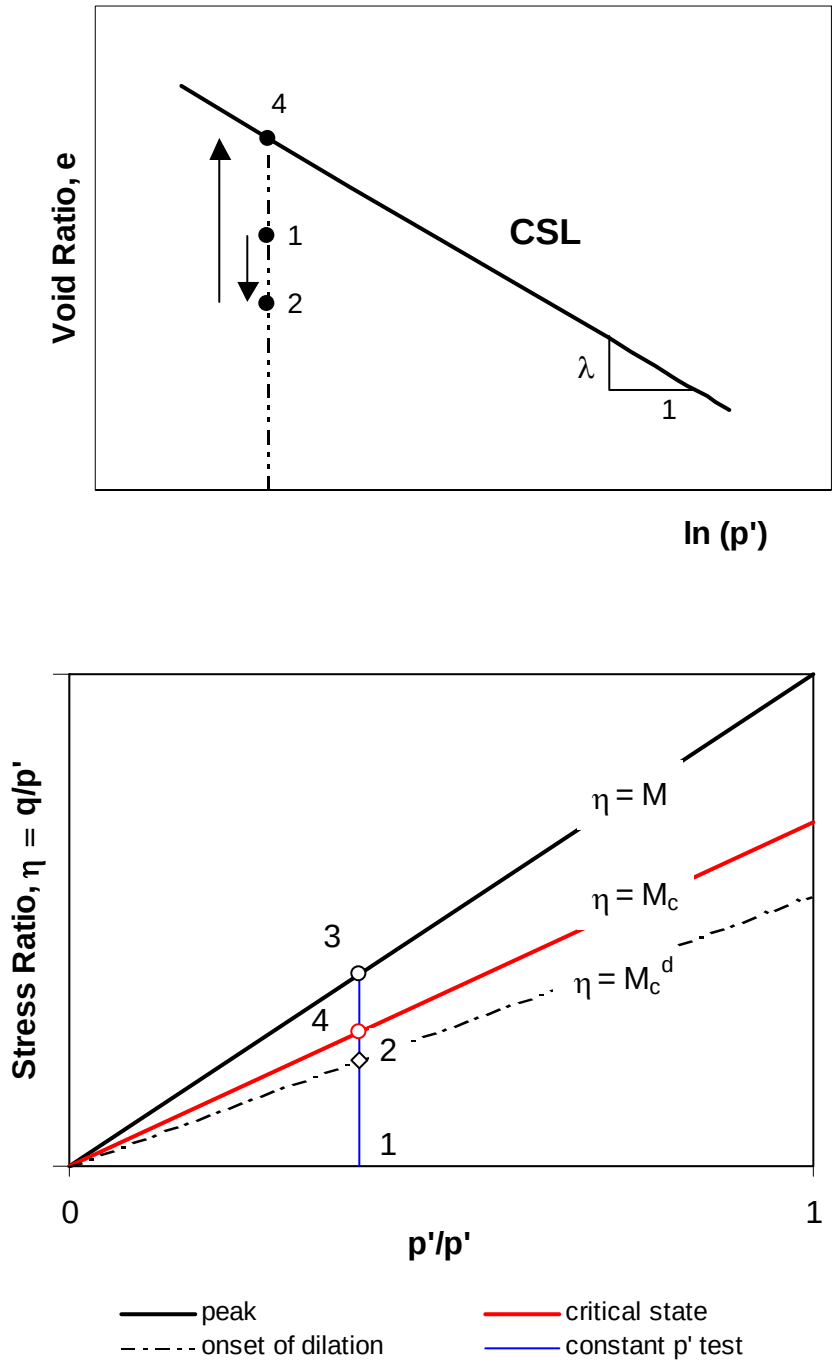

Figure 3-13. Definition of M_c^d, stress ratio at the onset of dilation (after Manzari and Dafalias, 1997) for a constant p′ test

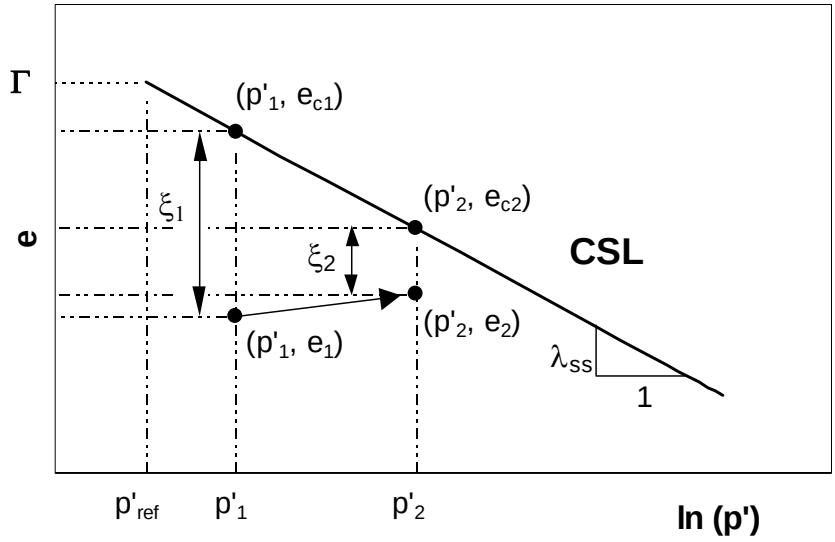

Figure 3-14. Illustration of the state parameter concept.

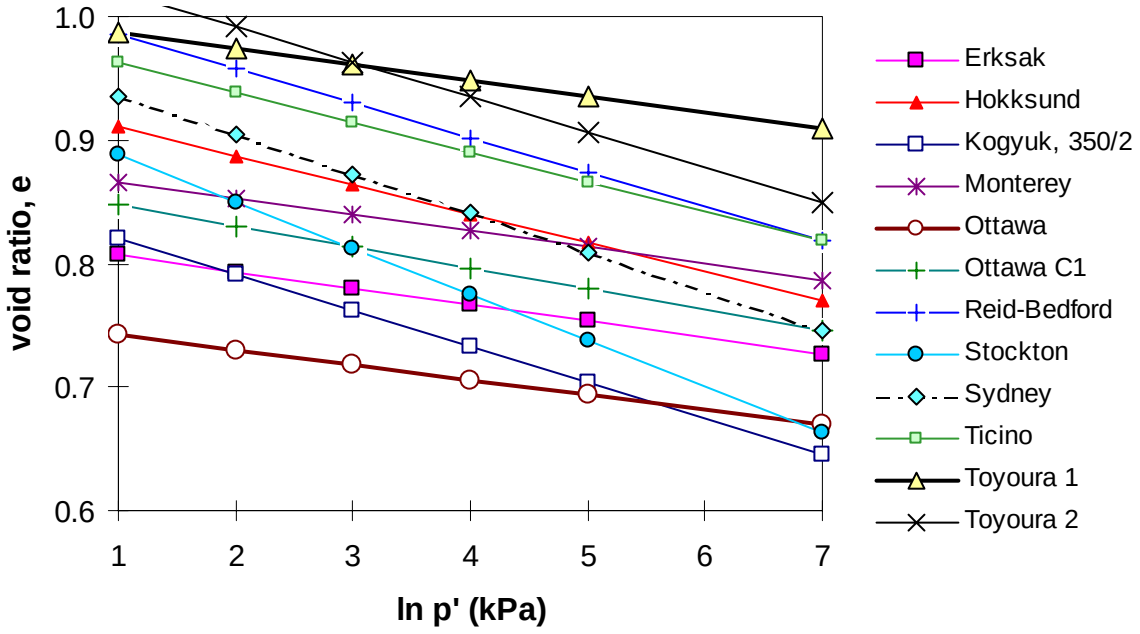

Figure 3-15. Critical State Lines for 12 sands

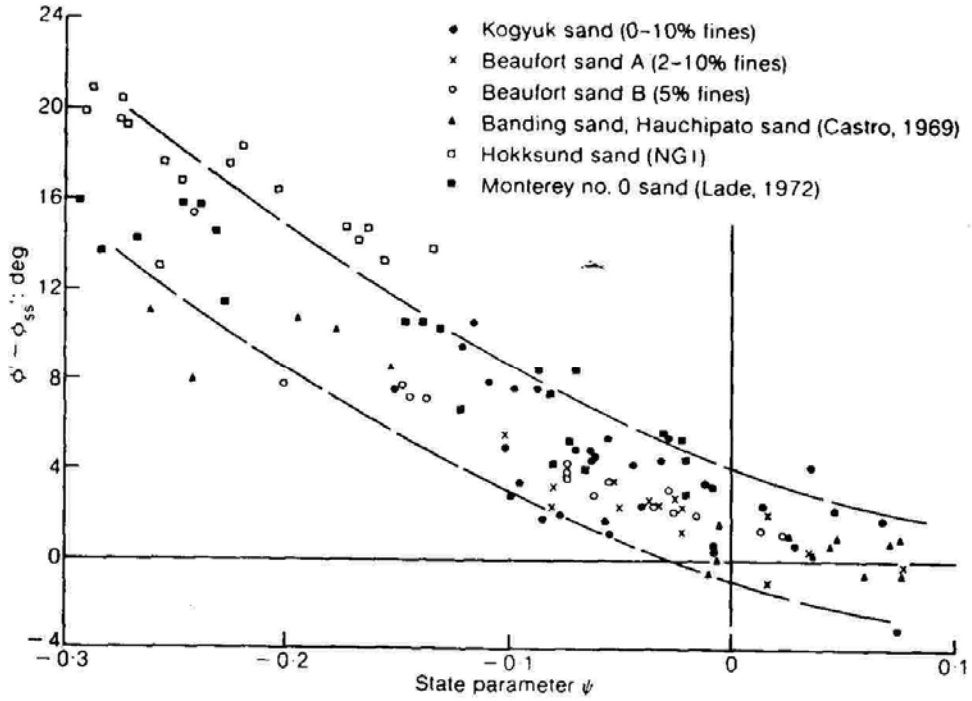

Fig. 15. $\phi' - \phi_{ss}'$ as a function of state parameter

Figure 3-16. The relationship between (ϕ_{max} - ϕ_{cv}) and state parameter for 13 sands (Been and Jefferies, 1985)

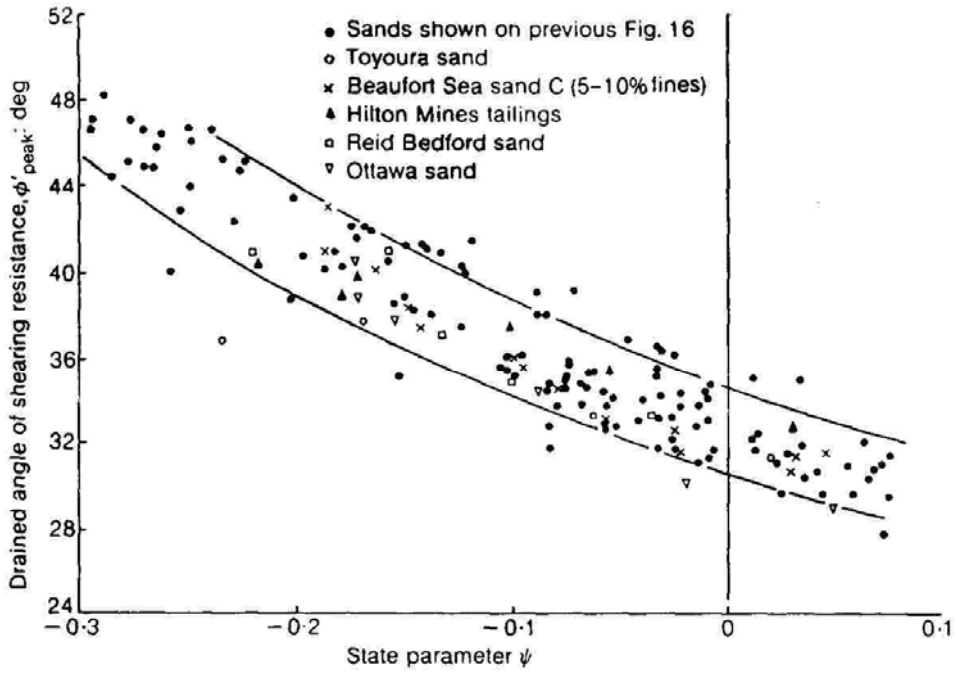

Fig. 7. Angle of shearing resistance for several sands from the Arctic, Europe, North and South America (revised Fig. 16, with additional data)

Figure 3-17. The relationship between ϕ_{max} and state parameter for 20 sands (Been and Jefferies, 1986)